Synthesis and structural, spectroscopic and magnetic characterization of iron(II) and iron(III) complexes of N-2-pyridinylcarbonyl-2-pyridinecarboximidate

Sigrid Wocadlo, Werner Massa

Fachbereich Chemie der Philipps Universität, Hans-Meerwein-Strasse, D-3550 Marburg (Germany)

and José-Vicente Folgado*

UIBCM, Departament de Química Inorgànica, Universitat de València, Dr. Moliner 50, 46100 Burjassot, València (Spain)

Abstract

One iron(II) complex of N-2-pyridinylcarbonyl-2-pyridinecarboximidate monoanion (bpca), $[Fe(bpca)_2] \cdot H_2O$ (**1**), and three iron(III) complexes, $[Fe(bpca)Cl_2(H_2O)] \cdot (CH_3)_2CO$ (**2**), $[Fe(bpca)_2](NO_3) \cdot 1.67H_2O$ (**3**), $[Fe(bpca)_2](ClO_4)$ (**4**), have been prepared and characterized by means of IR, UV–Vis and EPR spectroscopy and magnetic susceptibility measurements, where appropriate. The crystal structures of **1–3** have been determined from single crystal X-ray data, showing that the metallic ions are surrounded in all cases by distorted octahedral coordination spheres. From magnetic measurements it is evident that compounds **1** and **3** are practically in the low-spin state at room temperature, compound **2** is in the high-spin state in all the range of measured temperatures and compound **4** shows spin-crossover behaviour. Crystal data for **1**: space group $P2_1/c$, $a = 8.827(1)$, $b = 8.941(2)$, $c = 28.957(4)$ Å, $\beta = 95.90(1)°$, $Z = 4$; for **2**: space group $P2_1/c$, $a = 8.293(2)$, $b = 13.779(2)$, $c = 15.884(4)$ Å, $\beta = 98.22(1)°$, $Z = 4$; for **3**: space group $P\bar{1}$, $a = 8.840(1)$, $b = 10.713(1)$, $c = 14.989(1)$ Å, $\alpha = 71.16(1)$, $\beta = 73.43(1)$, $\gamma = 82.67(1)°$, $Z = 2$.

Introduction

In the past years we have demonstrated the ability of the N-donor tridentate rigid ligand bpca (N-2-pyridinylcarbonyl-2-pyridinecarboximidate anion) to coordinate transition metal ions such as Mn(II), Ni(II), Cu(II) or Zn(II) [1–6]. We studied monomeric $M(bpca)_2 \cdot nH_2O$ complexes where the MN_6 polyhedra can be considered as very distorted octahedra as a consequence of the rigidity of the tridentate ligand [3, 5]. Dealing with the Cu(II) ion, we were able to prepare compounds of formulation $Cu(bpca)X \cdot nH_2O$ (X = Cl, Br, NCS or CH₃COO) where the metallic center is pentacoordinate giving rise to monomeric (X = NCS or CH₃COO) [4, 6] or linear chain systems (X = Cl or Br) [2].

We are now studying the behaviour of the bpca ligand with the Fe(II) and Fe(III) ions. It seemed interesting to us to approach that study because of the well known possibility of both ions to be in the high-spin or low-spin state or to show spin-crossover behaviour [7, 8]. In this paper we report the synthesis and spectroscopic

and magnetic properties of four new iron–bpca compounds, including the crystal structure of three of them.

Experimental

Preparation of the compounds

The Hbpca free ligand was isolated as described in ref. 3.

$[Fe(bpca)_2] \cdot H_2O$ (1)

Solutions of Hbpca (227 mg, 1 mmol) in acetone (15 ml) and $FeSO_4 \cdot 7H_2O$ (139 mg, 0.5 mmol) in water (10 ml) were mixed with stirring. The pH of the resulting dark green solution was slowly changed to c. 7 (with aqueous NaOH) and a dark green microcrystalline solid appeared which was collected by filtration, washed with small portions of cold acetone and stored in a desiccator over silica gel. From the mother liquors, single crystals were obtained after several days showing the same colour and analysis as the powder samples. *Anal.* Found: C, 54.7; H, 3.5; N, 15.9. Calc. for $C_{24}H_{18}FeN_6O_5$: C, 54.8; H, 3.4; N, 16.0%.

---

*Author to whom correspondence should be addressed.

[Fe(bpca)Cl₂(H₂O)]·(CH₃)₂CO (2)

$[Fe(bpca)Cl_2(H_2O)] \cdot (CH_3)_2CO$ (2)

Solutions of Hbpca (227 mg, 1 mmol) in acetone (50 ml) and FeCl₃ (163 mg, 1 mmol) in water (3 ml) were mixed with stirring. From the resulting yellow–orange clear solution a yellow compound crystallized after a few days. The crystals were well formed and transparent in solution, but they became opaque when filtered off and finally disintegrated. Analytical data of freshly prepared samples are in agreement with an acetone content always less than one per mole of compound, all this implying that the solvent molecule easily evolves at room temperature.

[Fe(bpca)₂](NO₃)·1.67H₂O (3)

$[Fe(bpca)_2](NO_3) \cdot 1.67H_2O$ (3)

Solutions of Hbpca (227 mg, 1 mmol) in acetone (15 ml) and Fe(NO₃)₃·9H₂O (202 mg, 0.5 mmol) in water (5 ml) were mixed with stirring. The pH of the resulting orange solution was slowly changed to c. 3 (with aqueous NaOH) and the solution turned red–brown. After several days red–brown crystals suitable for X-ray analysis appeared and were separated by filtration. *Anal.* Found: C, 47.7; H, 3.3; N, 16.2. Calc. for $C_{24}H_{19.34}FeN_7O_{8.67}$: C, 48.0; H, 3.2; N, 16.3%.

[Fe(bpca)₂](ClO₄) (4)

$[Fe(bpca)_2](ClO_4)$ (4)

Solutions of Hbpca (227 mg, 1 mmol) in acetone (20 ml) and FeCl₃ (81 mg, 0.5 mmol) in water (5 ml) were mixed with stirring to give a clear orange solution the pH of which was slowly changed to c. 3 (with aqueous NaOH) and the solution turned red–brown. An excess of NaClO₄·H₂O dissolved in the minimum amount of water was added with stirring to the resulting solution and a red–brown microcrystalline solid appeared immediately, which was filtered off and washed with small portions of cold water and acetone. Recrystallization of this solid from water yielded red–brown small platelets with insufficient quality for X-ray single crystal analysis. *Anal.* Found: C, 47.6; H, 2.5; N, 13.8. Calc. for $C_{24}H_{16}ClFeN_6O_8$: C, 47.4; H, 2.6; N, 13.8%.

X-ray structural analyses of 1, 2 and 3

The crystal structure investigations were made on single crystals on an Enraf-Nonius CAD-4 diffractometer equipped with a low temperature device. The experimental crystallographic data are collected in Table 1. In all cases, the cell dimensions were refined from the θ angles of 25 high angle reflections determined as average from measurements in the positive and negative θ range. The measured sets of intensity data all showed few strong reflections and a large amount of rather weak reflections. In spite of the presence of Fe, a test measurement on a crystal of 3 yielded better data using Cu rather than Mo radiation, and the former was used

TABLE 1. Crystal and refinement data for 1, 2 and 3

	1	2	3
Space group	$P2_1/c$	$P2_1/c$	$P\bar{1}$
a (Å)	8.827(1)	8.293(2)	8.840(1)
b (Å)	8.941(2)	13.779(1)	10.713(1)
c (Å)	28.957(4)	15.884(4)	14.989(1)
α (°)			71.16(1)
β (°)	95.90(1)	98.22(1)	73.43(1)
γ (°)			82.67(1)
V (Å³)	2273(1)	1796(1)	1166(1)
Z	4	4	2
D_{calc} (g/cm³)	1.532	1.586	1.541
Crystal dimensions (mm)	0.28×0.25×0.14	0.20×0.20×0.08	0.25×0.15×0.06
Temperature (K)	293	208	293
Radiation, graphite monochromated	Cu Kα	Cu Kα	Cu Kα
μ (cm⁻¹)	57.6	98.0	52.1
Scan type	ω	ω	ω
Scan width (°)	0.9+0.14tgθ	1.0+0.14tgθ	0.8+0.14tgθ
	and 25% before and after each reflection for background determination		
Measuring range, θ (°)	2<θ<55	2<θ<55	2<θ<55
Octants	$h, k, \pm l$	$h, -k, \pm l$	$\pm h, \pm k, \pm l$
Reflections measured/unique	3072/2849	2555/2249	5214/3209
Reflections with $F_o > 3\sigma(F_o)$	2177	1867	2725
Absorption correction	numerical	DIFABS	none
Extinction correction, ϵ in $F_c^* = F_c/(1 + \epsilon F_c^2/\sin2\theta)^{0.25}$	5.1(3)×10⁻⁶	3.4(4)×10⁻⁶	1.4(6)×10⁻⁶
R/R_w	0.082/0.055	0.044/0.041	0.074/0.047
Goodness of fit	4.261	1.932	4.017
Largest shift/e.s.d., final cycle	0.06	0.001	0.001
Largest/lowest peak (e/Å³)	0.89/−0.54	0.35/−0.32	0.76/−0.41

therefore for all three crystals. The structures were solved using direct methods and difference Fourier syntheses. Refinements were carried out with the SHELXTL-PLUS program system [9] by weighted full-matrix least-squares methods with anisotropic temperature factors for all non-H atoms. Although in all structures the H atoms (except for disordered groups) could be located in difference Fourier maps, their positions were calculated (assuming C–H = 0.96 Å) using the riding model with group isotropic temperature factors. $\sum w(|F_o|-|F_c|)^2$ was minimized with $w = 1/[\sigma^2(F_o)]$ with $\sigma^2(F_o)$ from counting statistics. Atomic scattering factors and corrections for anomalous dispersion for the neutral atoms were taken from ref. 10. Final positional parameters and equivalent isotropic thermal parameters for non-hydrogen atoms are listed in Tables 2–4 and selected bond lengths and angles in

TABLE 2. Atomic fractional coordinates and equivalent isotropic thermal parameters (Å^2) for the non-hydrogen atoms in **1**

Atom	x	y	z	U_{eq}
Fe1	0.1068(2)	0.0561(2)	0.13364(5)	0.0380(6)
O1	0.0949(7)	0.2138(8)	0.0017(3)	0.070(3)
O2	0.2530(8)	−0.0646(9)	0.0116(2)	0.072(3)
O3	0.2439(7)	0.0815(9)	0.2709(2)	0.069(3)
O4	−0.0756(7)	0.0094(9)	0.2558(3)	0.086(4)
N1	0.0223(8)	0.2527(9)	0.1212(3)	0.039(3)
N2	0.1880(8)	−0.1446(9)	0.1287(3)	0.038(3)
N3	0.3087(8)	0.1384(9)	0.1530(3)	0.045(3)
N4	−0.0980(8)	−0.023(1)	0.1330(3)	0.044(3)
N5	0.1262(8)	0.056(1)	0.0683(2)	0.039(3)
N6	0.0934(8)	0.052(1)	0.1997(2)	0.046(3)
C11	−0.031(1)	0.351(1)	0.1493(4)	0.047(4)
C12	−0.102(1)	0.485(1)	0.1358(4)	0.058(5)
C13	−0.115(1)	0.520(1)	0.0896(5)	0.071(6)
C14	−0.059(1)	0.420(1)	0.0606(4)	0.064(5)
C15	0.011(1)	0.288(1)	0.0768(4)	0.045(4)
C16	0.081(1)	0.181(1)	0.0449(4)	0.047(4)
C21	0.202(1)	−0.252(1)	0.1604(4)	0.052(5)
C22	0.259(1)	−0.391(1)	0.1531(4)	0.067(6)
C23	0.301(1)	−0.423(1)	0.1094(5)	0.070(5)
C24	0.286(1)	−0.316(1)	0.0752(4)	0.056(5)
C25	0.227(1)	−0.179(1)	0.0864(4)	0.041(4)
C26	0.202(1)	−0.060(1)	0.0506(4)	0.047(4)
C31	0.415(1)	0.188(1)	0.1264(4)	0.051(4)
C32	0.550(1)	0.250(1)	0.1441(4)	0.061(5)
C33	0.584(1)	0.260(1)	0.1917(5)	0.072(6)
C34	0.477(1)	0.205(1)	0.2202(3)	0.059(5)
C35	0.341(1)	0.145(1)	0.1999(4)	0.046(4)
C36	0.220(1)	0.090(1)	0.2283(3)	0.047(4)
C41	−0.191(1)	−0.066(1)	0.0963(3)	0.051(4)
C42	−0.335(1)	−0.129(1)	0.1006(4)	0.058(5)
C43	−0.381(1)	−0.146(1)	0.1439(4)	0.062(5)
C44	−0.286(1)	−0.100(1)	0.1821(4)	0.055(5)
C45	−0.147(1)	−0.041(1)	0.1755(3)	0.043(4)
C46	−0.038(1)	0.009(1)	0.2159(4)	0.051(5)
O5[a]	0.485(1)	0.213(2)	0.0166(4)	0.152(9)
O6[b]	0.599(3)	0.571(4)	0.001(1)	0.15(2)

Occupation factors: [a]0.71(1), ; [b]0.29(1).

TABLE 3. Atomic fractional coordinates and equivalent isotropic thermal parameters (Å^2) for the non-hydrogen atoms in **2**

Atom	x	y	z	U_{eq}
Fe1	0.7524(1)	0.18569(6)	0.37999(5)	0.0235(3)
Cl1	0.5251(2)	0.1440(1)	0.28765(8)	0.0342(5)
Cl2	0.7239(2)	0.3496(1)	0.36523(8)	0.0338(5)
O1	0.8022(4)	−0.0745(2)	0.5164(2)	0.030(1)
O2	0.9596(5)	−0.0888(2)	0.3711(2)	0.033(1)
O3	0.9691(4)	0.2201(2)	0.4635(2)	0.030(1)
N1	0.6441(5)	0.1628(3)	0.4917(3)	0.025(2)
N2	0.9021(5)	0.1474(3)	0.2880(3)	0.023(1)
N3	0.8195(5)	0.0442(3)	0.4136(2)	0.021(1)
C11	0.5551(7)	0.2282(4)	0.5279(3)	0.033(2)
C12	0.4946(7)	0.2079(4)	0.6024(3)	0.040(2)
C13	0.5255(7)	0.1182(4)	0.6407(4)	0.038(2)
C14	0.6149(6)	0.0520(4)	0.6031(3)	0.028(2)
C15	0.6724(6)	0.0754(3)	0.5287(3)	0.025(2)
C16	0.7718(6)	0.0051(3)	0.4850(3)	0.022(2)
C21	0.9364(7)	0.2047(4)	0.2242(3)	0.029(2)
C22	1.0351(7)	0.1735(3)	0.1664(3)	0.034(2)
C23	1.0988(7)	0.0825(4)	0.1732(3)	0.036(2)
C24	1.0624(7)	0.0223(4)	0.2375(3)	0.029(2)
C25	0.9640(6)	0.0573(3)	0.2941(3)	0.024(2)
C26	0.9151(6)	−0.0058(3)	0.3647(3)	0.023(2)
O4	0.1674(5)	0.3836(3)	0.4693(3)	0.050(2)
C41	0.2411(7)	0.4072(4)	0.4121(4)	0.036(2)
C42	0.2577(7)	0.3413(4)	0.3403(4)	0.050(2)
C43	0.3212(8)	0.5036(4)	0.4120(4)	0.055(3)

Tables 5–7. In compound **1**, the crystal water molecule was found to be disordered over two neighbouring positions (distance of 2.12 Å) with occupation factors of 0.71(1) and 0.29(1), respectively, and its H atoms were not included in the final structure model refinement. In order to avoid evolution of the acetone molecule in compound **2**, the crystal studied was sealed inside a capillary tube containing mother liquor from the reaction vessel. Moreover, data were collected at 208 K to improve the results. Owing to the decomposition of the crystal at the end of the measurements, the necessary absorption correction had to be applied by means of DIFABS program [11]. Notwithstanding, the solvent molecule showed no disorder effects. Attempts to apply an absorption correction to the relatively small crystal of **3** did not lead to significant better results and were therefore omitted. In this structure, a complex disorder region including the nitrate anion and the crystal water molecules was observed: the nitrate anion is disordered over two alternative positions occupied with factors of 2/3 and 1/3, whereas one water molecule shows full occupation and the other has the occupation factor of 2/3. The atoms of the low occupied nitrate group together with one oxygen atom (O13) from the other group were refined with isotropic temperature factors.

Physical measurements

IR spectra (KBr pellets) were recorded in the 4000–250 cm^{-1} region using a Pye Unicam SP 2000

TABLE 4. Atomic fractional coordinates and equivalent isotropic thermal parameters (Å^2) for the non-hydrogen atoms in 3

Atom	x	y	z	U_{eq}
Fe1	−0.0688(1)	0.5924(1)	0.73582(8)	0.0378(4)
O1	0.2116(6)	0.5731(5)	0.4761(3)	0.060(2)
O2	−0.0863(6)	0.7009(5)	0.4577(3)	0.061(2)
O3	−0.1117(8)	0.6959(5)	0.9780(4)	0.099(3)
O4	−0.2572(8)	0.4539(5)	1.0253(4)	0.095(3)
N1	0.1452(6)	0.5146(5)	0.7281(4)	0.039(2)
N2	−0.2687(7)	0.6640(5)	0.7069(5)	0.045(2)
N3	−0.0043(7)	0.6066(5)	0.6002(4)	0.036(2)
N4	−0.0014(6)	0.7676(5)	0.7200(4)	0.038(2)
N5	−0.1525(6)	0.4137(5)	0.7894(4)	0.035(2)
N6	−0.1244(7)	0.5814(5)	0.8708(4)	0.044(2)
C11	0.216(1)	0.4600(7)	0.8033(5)	0.053(3)
C12	0.360(1)	0.3936(8)	0.7896(7)	0.065(4)
C13	0.4377(9)	0.3808(8)	0.7006(7)	0.066(4)
C14	0.3667(9)	0.4341(7)	0.6248(6)	0.052(3)
C15	0.2265(8)	0.5007(6)	0.6409(5)	0.038(3)
C16	0.1448(8)	0.5656(6)	0.5599(5)	0.038(3)
C21	−0.4078(9)	0.6831(7)	0.7693(6)	0.056(3)
C22	−0.543(1)	0.7341(8)	0.7405(7)	0.069(4)
C23	−0.533(1)	0.7670(8)	0.6424(7)	0.072(4)
C24	−0.394(1)	0.7449(7)	0.5773(6)	0.058(3)
C25	−0.2662(9)	0.6961(6)	0.6104(5)	0.040(3)
C26	−0.1085(9)	0.6684(6)	0.5462(6)	0.043(3)
C31	0.0612(8)	0.8615(7)	0.6373(6)	0.050(3)
C32	0.1085(9)	0.9790(7)	0.6374(6)	0.061(3)
C33	0.101(1)	1.0027(8)	0.7234(7)	0.067(4)
C34	0.0346(9)	0.9093(7)	0.8081(6)	0.066(4)
C35	−0.0148(9)	0.7947(7)	0.8056(6)	0.049(3)
C36	−0.091(1)	0.6877(7)	0.8962(6)	0.063(4)
C41	−0.1566(8)	0.3352(6)	0.7393(5)	0.041(3)
C42	−0.2220(9)	0.2099(7)	0.7849(6)	0.051(3)
C43	−0.284(1)	0.1709(7)	0.8852(6)	0.079(4)
C44	−0.282(1)	0.2555(7)	0.9379(6)	0.072(4)
C45	−0.2118(9)	0.3768(7)	0.8884(5)	0.049(3)
C46	−0.204(1)	0.4734(8)	0.9377(6)	0.059(3)
N10[a]	0.6191(8)	0.0802(6)	0.6192(6)	0.126(8)
O11[a]	0.6875(8)	0.1313(6)	0.5465(6)	0.188(9)
O12[a]	0.4776(8)	0.0918(6)	0.6685(6)	0.182(9)
O13[a]	0.6971(8)	0.0137(6)	0.6626(6)	0.162(6)
N20[b]	0.450(1)	0.0329(9)	0.1925(7)	0.077(6)
O21[b]	0.397(1)	0.1255(9)	0.1020(7)	0.139(8)
O22[b]	0.557(1)	−0.0212(9)	0.1978(7)	0.099(7)
O23[b]	0.341(1)	0.0233(9)	0.2659(7)	0.051(4)
O7	0.8853(9)	0.9042(6)	0.0669(5)	0.133(4)
O14[a]	0.598(1)	0.009(1)	0.1295(7)	0.138(5)

Occupation factors: [a] 0.6667, [b] 0.3333 (isotropic U).

TABLE 5. Selected bond distances (Å) and angles (°) for 1

Distances			
Fe–N1	1.929(8)	Fe–N2	1.943(8)
Fe–N3	1.957(7)	Fe–N4	1.941(7)
Fe–N5	1.918(7)	Fe–N6	1.929(7)
Angles			
N1–Fe–N2	165.1(3)	N1–Fe–N3	91.9(3)
N1–Fe–N4	89.4(3)	N1–Fe–N5	83.7(4)
N1–Fe–N6	98.0(4)	N2–Fe–N3	92.1(3)
N2–Fe–N4	90.7(3)	N2–Fe–N5	81.6(3)
N2–Fe–N6	96.8(4)	N3–Fe–N4	163.9(3)
N3–Fe–N5	96.4(3)	N3–Fe–N6	82.5(3)
N4–Fe–N5	99.6(3)	N4–Fe–N6	81.4(3)
N5–Fe–N6	178.1(3)		

TABLE 6. Selected bond distances (Å) and angles (°) for 2

Distances			
Fe–Cl1	2.290(2)	Fe–Cl2	2.280(2)
Fe–O3	2.129(4)	Fe–N1	2.124(4)
Fe–N2	2.115(4)	Fe–N3	2.076(4)
Angles			
Cl1–Fe–Cl2	96.84(6)	Cl1–Fe–O3	177.7(1)
Cl1–Fe–N1	95.2(1)	Cl1–Fe–N2	90.3(1)
Cl1–Fe–N3	95.5(1)	Cl2–Fe–O3	84.79(9)
Cl2–Fe–N1	100.6(1)	Cl2–Fe–N2	103.8(1)
Cl2–Fe–N3	167.6(1)	O3–Fe–N1	86.1(1)
O3–Fe–N2	87.7(2)	O3–Fe–N3	83.0(1)
N1–Fe–N2	154.2(2)	N1–Fe–N3	77.0(2)
N2–Fe–N3	77.3(2)		

TABLE 7. Selected bond distances (Å) and angles (°) for 3

Distances			
Fe–N1	1.955(6)	Fe–N2	1.943(6)
Fe–N3	1.908(5)	Fe–N4	1.963(6)
Fe–N5	1.971(6)	Fe–N6	1.908(5)
Angles			
N1–Fe–N2	163.7(3)	N1–Fe–N3	80.9(3)
N1–Fe–N4	92.6(2)	N1–Fe–N5	89.5(2)
N1–Fe–N6	97.3(3)	N2–Fe–N3	83.2(3)
N2–Fe–N4	92.3(3)	N2–Fe–N5	89.9(2)
N2–Fe–N6	98.7(30)	N3–Fe–N4	95.7(2)
N3–Fe–N5	99.9(2)	N3–Fe–N6	177.4(3)
N4–Fe–N5	164.4(2)	N4–Fe–N6	82.4(2)
N5–Fe–N6	82.0(2)		

spectrophotometer. Diffuse reflectance and solution electronic spectra were recorded on a Perkin Elmer Lambda 9 UV/VIS/NIR spectrophotometer. EPR spectra (20–300 K) were recorded on a Bruker ER 200D (X-band) spectrometer, equipped with a variable temperature device. Magnetic susceptibility measurements were obtained using a pendulum-type apparatus equipped with a helium cryostat.

Results and discussion

Crystal structures

Figures 1–3 show XP diagrams [9] of the molecular structures of compounds 1–3, respectively, with the labelling scheme. In 1, the Fe(II) ion is hexacoordinated via the six nitrogen atoms from the two bpca ligands, in a geometry that can be regarded as very distorted octahedral. This distortion is due to the rigidity of the bpca ligand and is well documented in the deviation
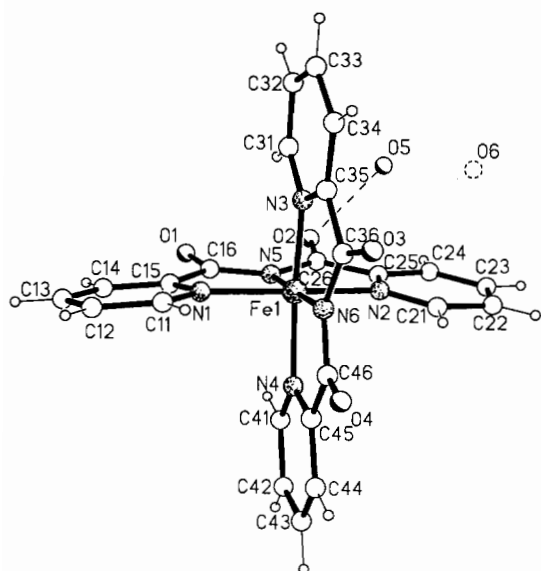
Fig. 1. XP drawing of compound **1**, showing the two alternative positions of the disordered water molecule with the weakly occupied position dashed.
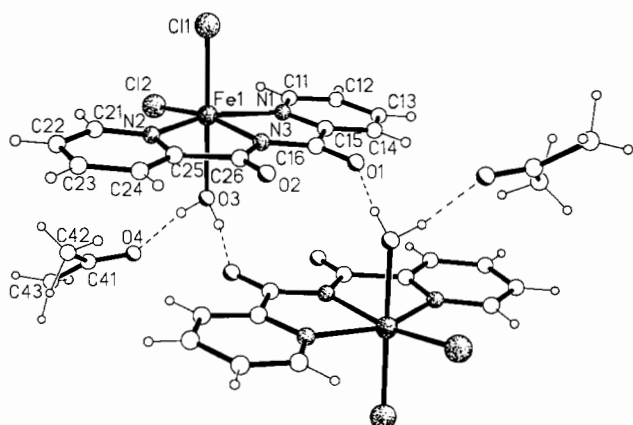
Fig. 2. XP drawing of compound **2**, showing the 'dimeric' unit formed by the hydrogen bond system.

Fig. 3. XP drawing of compound **3**, showing the two alternative positions of the disordered nitrate ion with the weakly occupied position dashed.

of the angles N1–Fe–N2 and N3–Fe–N4 (165.1 and 163.9°, respectively) from linearity which rests almost preserved in the N5–Fe–N6 axis (178.1°). The Fe–N distances are practically equal, ranging from 1.918(7) to 1.957(7) Å and are similar to those observed in other low-spin Fe(II)–nitrogen complexes [8]. The set of N(1), N(2), N(5) and N(6) atoms, together with the set N(3), N(4), N(5) and N(6) nicely define planes (within ±0.03 Å), where the iron atom is included (at 0.01 Å), which are perpendicular (89.7°). The adaptation of the bpca ligands to the pseudooctahedral geometry of the FeN_6 polyhedra requires deformations of the ligand framework. Both ligands are non-equivalent and neither of them can be considered planar. Although the pyridyl units can be considered planar, within experimental error, the planes of both six-membered

rings are inclined 3.5° in one ligand and 12.4° in the other. Furthermore, it is to be noted that the values of the angles around the carbon atoms involved in the carbonyl groups significantly differ from the idealized 120° value, as previously observed in other bpca complexes [2–6]. Finally, the crystal packing is achieved by intermolecular hydrogen bonding. Indeed the water molecule O5 is hydrogen bonded to the carbonyl O2 atom (at 3.21 Å) and to the inversion centre related O2' atom (at 2.86 Å), joining the neutral complex molecules two by two.

The hexacoordination of Fe(III) ions in compound **2** is achieved by means of the three nitrogen atoms from the bpca ligand, two chlorine atoms and the oxygen atom from the water molecule. Severe distortions from the idealized octahedral geometry, both in angles and distances, are present in this case due to the internal strain of the organic ligand and the differences in the nature of the coordinated atoms. Iron–ligand distances are all in the range expected for high-spin Fe(III) complexes [12–14]. Owing to the smaller size of the O3 ligand as compared to the *trans* Cl1 atom, the O3–Fe–L angles (L=N1, N2, N3 and Cl2) are significantly lower than 90°, those four atoms being practically coplanar and the Fe atom lying 0.17 Å over their best mean plane. Again the crystal packing is achieved by means of intermolecular hydrogen bonding. The coordinated water molecule is simultaneously hydrogen bonded to the oxygen atom from the acetone molecule (O3...O4=2.783 Å) and to the carbonyl O1 oxygen atom (O3...O1=2.783 Å) from the bpca ligand of a neighbouring complex molecule, giving rise to the formation of a centrosymmetric 'dimeric' unit as shown in Fig. 2.

The geometry of the FeN$_6$ polyhedra in **3** can be viewed as very distorted and slightly compressed octahedral. Indeed, in the compression N3–Fe–N6 axis the iron–nitrogen distances are 1.908(5) Å, whereas in the 'equatorial plane' they are 1.96(2) Å. This compression is the result of the rigid structure of the bpca ligands, which enforces shorter metal–N(central) bond distances, as previously observed in the Cu(II) and Mn(II) bpca complexes [3, 5]. It is to be noted that the average Fe–N bond length in this complex (1.94 Å) is significantly shorter than that found in compound **2** (2.11 Å). This is directly correlated with the different spin state of Fe(III) in both compounds. As we will see later on, compound **3** is basically in the low-spin state even at room temperature and thus shorter bond distances than in the high-spin state are expected [14]. The N(1), N(2), N(3) and N(6) atoms and N(3), N(4), N(5) and N(6) atoms define nicely two planes (maximum deviation of 0.05/0.02 Å, respectively) which are perpendicular (89.8°), and the iron atom lies practically within both planes (displacements of 0.01/0.02 Å, respectively). As in **1**, neither of the two ligands can be considered planar and the values of the angles around the carbon atoms involved in the carbonyl groups are severely far ($\pm 11°$) from the idealized 120° value. As indicated in 'Experimental', the nitrate group was found to be disordered. Since the complex cation is well defined and the nitrate anion is not of primary interest, the disorder problem was not pursued further.

Infrared and electronic spectra

The IR spectra of the studied compounds are dominated by the great number of peaks due to the presence of the bpca ligand. Among them, is to be noted a very strong peak appearing in the range 1710–1725 cm^{-1} assignable to the C=O stretching vibrations of bpca carbonyl groups [1]. Peaks of weak–medium intensity due to the O–H stretching vibrations of water molecules are present in the IR spectrum of **1** (3300–3650 cm^{-1}, broad), **2** (3500 cm^{-1} sharp, 3600 cm^{-1} sharp) and **3** (broad absorption between 3200–3700 cm^{-1} with two well defined maxima at 3330 and 3580 cm^{-1}), which are absent in **4** according to the formulation. Moreover, bands due to the inorganic counterions in **3** and **4** appeared unsplit, thus indicating the non-coordination of these groups [15]. Notwithstanding, the IR spectrum of **2** clearly shows an intense band centered at 375 cm^{-1} which is not present in the other cases. This can be unambiguously assigned to the Fe–Cl stretching vibrations, according to the literature [16–18]. It is also to be noted that the IR spectrum of **2** does not show any band assignable to the acetone group, this implying that the studied powdered samples of this specimen do not contain that solvate molecule and must be reformulated in the following as [Fe(bpca)Cl$_2$(H$_2$O)].

Both the reflectance and solution (chloroform or acetone) electronic spectra of compound **1** show an intense band at 20 700 cm^{-1}, together with a weak one at 15 300 cm^{-1} with a shoulder at 13 500 cm^{-1}. The former must be due to a metal-to-ligand charge-transfer transition between the t$_{2g}^6$ state and empty π^* orbitals of the bpca ligand, as observed usually in low-spin N-heterocycle–Fe(II) complexes, and the latter to d–d transitions between the fundamental singlet state and the low lying triplets [19]. On the other hand, spectra of the Fe(III) complexes show only intense bands above 19 000 cm^{-1} in **2** and 17 000 cm^{-1} in **3** and **4** that can be assigned to ligand-to-metal charge-transfer transitions [19].

EPR spectra and magnetic measurements

Any significant signal is observed in the EPR spectra of the Fe(II) complex **1** from room temperature down to 20 K. Moreover, the effective magnetic moment per Fe(II) ion is 2.09 BM at 290 K and slowly decreases to a value of 1.53 BM at 20 K. These values are significantly lower than that of 4.9 BM expected for four unpaired electrons. Consequently, complex **1** must be considered being in the low-spin state although with a residual paramagnetic (high-spin) fraction (estimated from $\chi_M = x$ ($8N\beta^2/kT$)) of 0.18 at 290 K and 0.10 at 20 K. Such residuals are usually found even in the iron(II) complexes showing abrupt discontinuous high-spin to low-spin transitions, and depend on several distinct factors [8].

The room temperature EPR spectrum of powdered samples of **2** (Fig. 4) consists of a broad (≈ 700 Gauss peak-to-peak) intense signal centered at $g_{eff} = 4.28$ and a weak one at $g_{eff} \approx 2$, remaining practically unchanged when lowering the temperature. These features are those expected for high-spin Fe(III) ions in strongly distorted octahedral environments leading to large zero-field splitting ($D > h\nu = 0.3$ cm^{-1} in X band) of the $^6A_{1g}$ state [20, 21], and are in agreement with the structural findings. Consequently, the room temperature μ_{eff} of **2** is 5.98 BM (as expected for five unpaired electrons per Fe atom) and the molar susceptibility nicely follows a Curie–Weiss law with $\theta = -5.7$ K. This small negative θ value must be accounted in terms of the zero-field splitting rather than of weak antiferromagnetic intermolecular interactions [22].

Very different EPR and magnetic behaviour is showed by the other Fe(III) complexes **3** and **4** when compared to **2**. The room temperature μ_{eff} of **3** is 3.00 BM, decreases to 2.20 BM at 240 K and then goes smoothly to a value of 1.80 at 20 K. These values indicate that **3** is practically in the low-spin state ($^2T_2$) below c. 240 K, since values of 2.1–2.3 BM are usual for $S = 1/2$ states with some degree of orbital contributions [21,
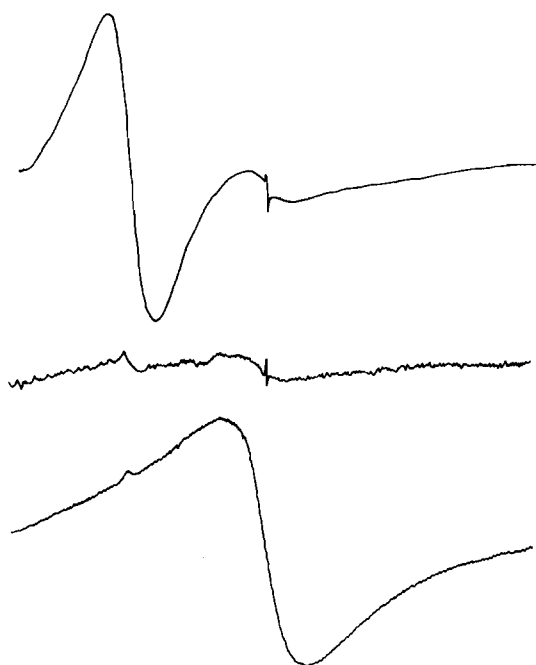
Fig. 4. X-band room temperature EPR powder spectra of compounds 2 (top), 3 (middle) and 4 (bottom). The magnetic field scans go from 0 to 7000 Gauss, and the narrow signals correspond to DPPH ($g = 2.003$).

23, 24]. Notwithstanding, if we calculate the high-spin population percentage using the spin-only approximation ($\chi_M = x(35N\beta^2/3kT) + (1 - x)(N\beta^2/kT)$) we can consider that the 'pure' low-spin state must be achieved around 100 K ($\mu_{eff} \leqslant 2.00$ BM, $x \leqslant 0.03$). On the other hand, the μ_{eff} of 4 changes continuously from a value of 4.4 BM at 290 K to 3.3 BM at 20 K, which indicates it is undergoing a continuous high-spin to low-spin transition which is not totally accomplished even at 20 K. The high-spin population percentage at 20 and 290 K can be estimated as 25 and 51%, respectively. Shown in Fig. 4 are typical room temperature EPR powder spectra of compounds 3 and 4. Weak broad lines at $g_{eff} \approx 4.3$ and $g_{eff} \approx 2$ are observed which can be interpreted as resulting from transitions in the $S = 5/2$ electronic configuration [21, 23]. It is worth noting the higher relative intensity of these signals in compound 4 when compared to 3, according to the greater fraction of high-spin population in 4 as found in the susceptibility measurements (0.51 in front of 0.19). Also in accord to the magnetic findings, the high-spin EPR signals are practically absent in the spectra of 3 below 100 K, whereas they remain in the spectra of 4 even at lower temperatures. On the other hand, we were not able to observe narrow signals centered at $g_{eff} \approx 2$, corresponding to transitions in the $S = 1/2$ state, which have been seen in the well studied spin-crossover dithio and diselenocarbamate–Fe(III) complexes [21, 23]. This might be due to the presence in our compounds of

fast spin lattice relaxation pathways making signals of the ground doublet state unobservable above 20 K.

As a conclusion it can be stated that the coordination of only one bpca ligand to the Fe(III) ion is not enough to cause a field enforcing the spin pairing (compound 2) which is accomplished when two bpca ligands are coordinated to the metallic ions (compounds 1, 3 and 4). Another fact to note when comparing compounds 3 and 4 (although the crystal structure of the latter is lacking) is that subtle changes in the coordination geometry due to crystal packing (different counterions, water molecules) may induce sensitive differences in the spin-crossover behaviour.

Supplementary material

Tables of anisotropic thermal parameters, hydrogen atoms parameters, complete bond lengths and angles, and observed and calculated structural factors can be obtained from the authors upon request.

Acknowledgement

References

1 J. V. Folgado, E. Escrivá, A. Beltrán and D. Beltrán, *Transition Met. Chem. (Weinheim, Ger.)*, 12 (1987) 306.
2 J. V. Folgado, E. Coronado, D. Beltrán, R. Burriel, A. Fuertes and C. Miravitlles, *J. Chem. Soc., Dalton Trans.*, (1988) 3041.
3 D. Marcos, R. Martínez, J. V. Folgado, A. Beltrán, D. Beltrán and A. Fuertes, *Inorg. Chim. Acta*, 159 (1989) 11.
4 J. V. Folgado, E. Martínez, A. Beltrán, D. Beltrán, A. Fuertes and C. Miravitlles, *Polyhedron*, 8 (1989) 1077.
5 D. Marcos, J. V. Folgado, D. Beltrán, M. T. Prado-Gambardella, S. H. Pulcinelli and R. H. Almeida-Santos, *Polyhedron*, 9 (1990) 2699.
6 G. Madariaga, F. J. Zúñiga, T. Rojo and J. V. Folgado, *Acta Crystallogr., Sect. C*, 47 (1991) 1632.
7 P. Gütlich, *Struct. Bonding (Berlin)*, 44 (1981) 83.
8 E. König, G. Ritter and S. K. Kulshreshtha, *Chem. Rev.*, 85 (1985) 219.
9 G. M. Sheldrick, *SHELXTL-PLUS*, Release 4.0 for Siemens R3 Crystallographic Research System, Siemens Analytical X-Ray Instruments, Inc. Madison, WI, USA, 1989.
10 *International Tables for X-Ray Crystallography*, Vol. 4, Kynoch, Birmingham, UK, 1974.
11 N. Walker and D. Stewart, *Acta Crystallogr., Sect. A*, 39 (1983) 158.
12 E. C. Constable, M. S. Kahn, J. Lewis, M. C. Liptrot and P. R. Raithby, *Inorg. Chim. Acta*, 181 (1991) 207.
13 A. Bonardi, C. Carini, C. Merlo, C. Pelizzi, G. Pelizzi, P. Tarasconi, F. Vitali and F. Cavatorta, *J. Chem. Soc., Dalton Trans.*, (1990) 2771.

14 Y. Maeda, H. Oshio, K. Toriumi and Y. Takashima, *J. Chem. Soc., Dalton Trans.*, (1991) 1227.

15 K. Nakamoto, *Infrared and Raman Spectra of Inorganic and Coordination Compounds,* Wiley, New York, 4th edn., 1986, p. 130.

16 J. D. Walker and R. Poli, *Inorg. Chem., 28* (1989) 1793.

17 J. C. Daran, Y. Jeannin and L. M. Martin, *Inorg. Chem., 19* (1980) 2935.

18 H. J. Goodwin, M. McPartlin and H. A. Goodwin, *Inorg. Chim. Acta, 25* (1977) L74.

19 A. B. P. Lever, *Inorganic Electronic Spectroscopy,* Elsevier, New York, 2nd edn., 1986, Chs. 5 and 6.

20 A. Bencini and D. Gatteschi, in G. A. Melson and B. N. Figgis (eds.), *Transition Metal Chemistry,* Vol. 8, Marcel Dekker, New York, 1982, p. 1.

21 (a) E. Gelerinter, N. V. Duffy, W. Dietzsch, T. Thanyasiri and E. Sinn, *Inorg. Chim. Acta, 177* (1990) 185; (b) C. Flick, E. Gelerinter, J. B. Zimmerman and N. V. Duffy, *Inorg. Chem., 15* (1976) 2945.

22 G. R. Hall and D. N. Hendrikson, *Inorg. Chem., 15* (1976) 607.

23 W. Dietzsch, N. V. Duffy, E. Gelerinter and E. Sinn, *Inorg. Chem., 28* (1989) 3079.

24 M. D. Timken, S. R. Wilson and D. H. Hendrikson, *Inorg. Chem., 24* (1985) 3457.